Journal of the European Ceramic Society 21 (2001) 2621–2628

www.elsevier.com/locate/jeurceramsoc

Ceramic microwave antennas for mobile applications

I.S. Ghosh*, A. Hilgers, T. Schlenker, R. Porath

Philips GmbH Forschungslaboratorien, Weißhausstr. 2, 52066 Aachen, Germany

Abstract

Due to their medium to high permittivity values, ceramic microwave materials are attractive as building blocks for miniaturised antenna solutions. Further advantages are low dielectric losses and an excellent temperature stability of standard ceramic materials. Yet, the permittivity of the ceramic material also has a strong influence on the radiation efficiency and bandwidth of the antenna. This implies that in the design process a suitable compromise has to be found between the degree of miniaturisation on the one hand and the antenna efficiency and bandwidth on the other. We describe two approaches towards efficient miniaturised ceramic microwave antennas: the dielectric resonator antenna (DRA) with partial metallisation and the shorting post patch antenna. We focus on design steps taken to ensure both a high degree of miniaturisation and high values of the radiation efficiency, the choice of the ceramic material and the experimental performance of the antennas. © 2001 Published by Elsevier Science Ltd. All rights reserved.

1. Introduction

Compared with their conventional counterparts (e.g. rod or whip antennas) ceramic antenna solutions for mobile telecommunications offer the possibility to drastically decrease the antenna size. Due to the wavelength scaling with $(\varepsilon_r)^{-1/2}$ the larger the permittivity of the material the smaller the antenna dimensions can be made. Conventional antenna solutions are usually exterior to the mobile device which can lead to reliability problems (e.g. the antenna breaking off the device if it falls onto the ground). With an internal antenna this problem could be avoided. Moreover, it would be highly desirable to mount the antenna in a surface mount process (SMD). This would substantially reduce the costs of the antenna placement onto the PCB of the mobile device.

We will introduce and discuss the key parameters characterising the antenna performance. From these we will deduce the requirements imposed both on the dielectric material serving as the building block of the antenna and the metal used as antenna metallisation. The main part of this paper concentrates on two ceramic antenna types: the dielectric resonator antenna (DRA) and the shorting post patch antenna. We will introduce the design rationale and discuss the antenna performance in detail.

* Corresponding author. Tel.: +49-2842-95-4040; fax: +49-2842-95-4379.

E-mail address: indra.ghosh@klf.siemens.de (I.S. Ghosh).

2. Key antenna parameters and requirements for the ceramic material

The key antenna parameters are the resonance frequency f, the return loss, Q and bandwidth, efficiency η, directivity D and gain G. Generally, the quality factor Q of a resonator is defined as the ratio of oscillating power over dissipated power. For a ceramic antenna, the dissipated power is the sum the radiated power P_{rad}, the power dissipated in the metal electrodes (i.e. due to ohmic losses) P_{cond}, and the power dissipated due to dielectric losses in the ceramic material P_{diel}. Therefore,

$$\frac{1}{Q} = \frac{1}{Q_{\text{rad}}} + \frac{1}{Q_{\text{cond}}} + \frac{1}{Q_{\text{diel}}}.$$

The antenna bandwidth is defined as the frequency range over which the return loss of the antenna is larger than a certain value (e.g. 10 dB). It is directly linked to the quality factor of an antenna. For example, the 10 dB bandwidth of an antenna (BW) is linked to the quality factor Q via

$$BW = \frac{f}{\sqrt{2}Q}.$$

The antenna efficiency η is defined as the ratio of the radiated power over the total input power which is fed to the antenna. The antenna efficiency can be expressed in terms of the quality factors:

0955-2219/01/$ - see front matter © 2001 Published by Elsevier Science Ltd. All rights reserved.
PII: S0955-2219(01)00327-2

$$\eta = \frac{1}{1 + Q_{\text{rad}}/Q_{\text{cond}} + Q_{\text{rad}}/Q_{\text{diel}}}.$$

This implies that Q_{rad} needs to be small compared with both Q_{diel} and Q_{cond} to come up with efficiencies close to one. As expected, this relates to radiation losses being the dominant loss mechanism.

The directivity D relates to the radiation pattern of the antenna: it is defined as the ratio of the radiated power in a certain direction over the average radiated power per unit solid angle,

$$D(\theta, \varphi) = \frac{4\pi \ \mathrm{d}P_{\text{rad}}(\theta, \varphi)/\mathrm{d}\Omega}{P_{\text{rad}}}.$$

For example, for an ideal half-wavelength dipole made of a conducting wire the maximum directivity is 1.64 = +2.15 dBi where 0 dBi relates to an isotropic radiator. The radiation pattern is isotropic perpendicular to the axis of the dipole and has nodes along the axis of the dipole.

Finally, the antenna gain G is defined as the product of the antenna efficiency and directivity. Therefore, G is a measure of the real antenna performance including all loss mechanisms and the radiation pattern.

As mentioned above, the size of a ceramic patch antenna decreases like $\varepsilon_r^{-1/2}$ with increasing values of the permittivity ε_r of the ceramic material. This suggests that a ceramic antenna can be made arbitrarily small by enhancing the permittivity. However, when taking into account the radiation properties a different scenario arises: Fig. 1 shows both the physical length and the radiation efficiency as a function of the permittivity of the ceramic material of a half-wavelength patch antenna at 900 MHz (width = length/1.5, height = 4 mm). In the cavity model calculations dielectric losses have been neglected and the conductivity of the metallisations was similar to the dc-conductivity of a typical pure silver paste used to metallise our ceramic blocks (i.e. $\sigma = 3{\cdot}10^7$ S/m). As expected, the length drops as ε_r increases. Yet, the efficiency is also a decreasing function of the permittivity. This is due to the reflection of the microwave power at the interface between the ceramic antenna substrate and air, which increases as ε_r rises. For reasonable values of η (> 0.7) only materials with $\varepsilon_r < 30$ can be used.

For the antenna types discussed below the Q values are of the order of 100. For $\eta = 0.7$ and $Q = 100$ this results in $Q_{\text{rad}} = 143$ and $Q_{\text{cond}} = 333$. For the dielectric losses not further depressing the antenna efficiency $\tan\delta = 10^{-4}$ at 1 GHz is sufficient.

W.r.t. the temperature stability of the permittivity the following reasoning can be applied: As the antenna resonance frequency $f \propto \varepsilon_r^{-1/2}$,

$$\frac{\delta f}{f} = -\frac{1}{2}\frac{\delta\varepsilon_r}{\varepsilon_r}.$$

If the 10 dB bandwidth of the antenna corresponds to ≈1.5 times the application bandwidth, then the reso-

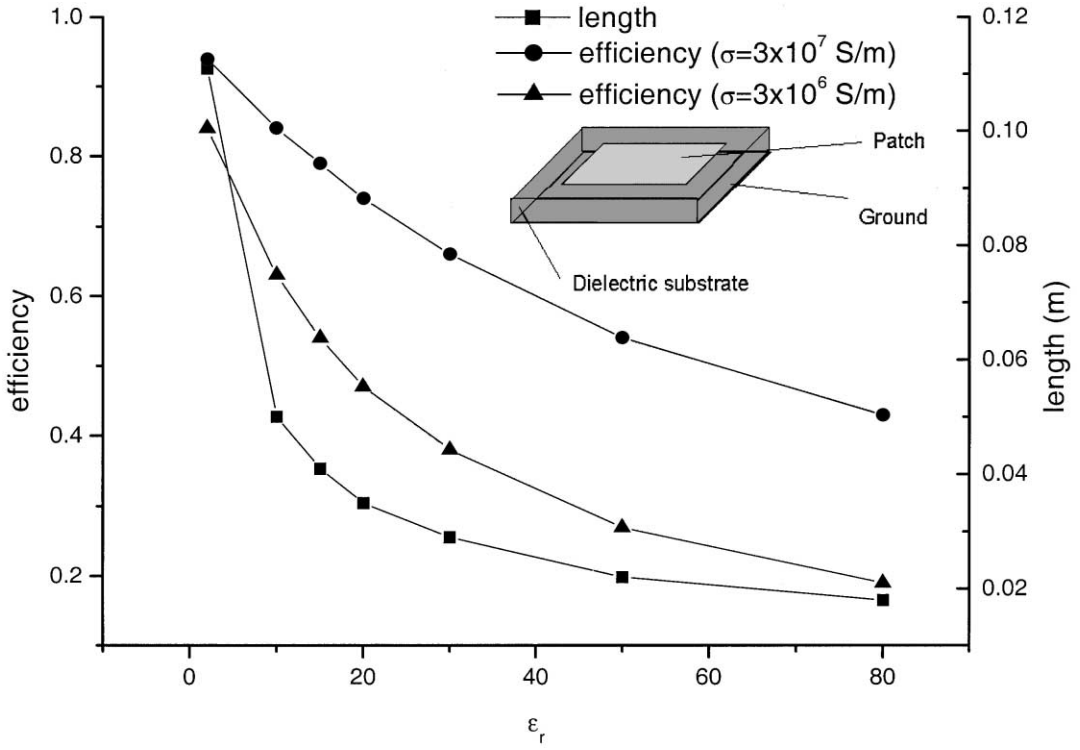

Fig. 1. Length and radiation efficiency of a patch antenna as a function of the permittivity of the dielectric substrate. The resonance frequency is 900 MHz, the antenna width is two thirds of its length and the substrate height is 4 mm.

nance frequency of the antenna must not shift by more than a quarter of the application bandwidth within the temperature range from −40 to +85 °C. With $Q = 100$ this corresponds to $\delta f/f < 1.2 \times 10^{-3}$ and $\delta\varepsilon_r/\varepsilon_r < 2.4 \times 10^{-3}$ over the same temperature range. This corresponds to $\delta\varepsilon_r/\varepsilon_r < 19$ ppm/°C for the ceramic material. Consequently, NP0 materials have to be used as building block for ceramic antennas.

For the antennas described below we used an NP0-K17 ceramic material ($Ca_{0.05}$ $Mg_{0.95}$ Ti O_3) as the building block for our antennas. The material parameters have been determined at 9 GHz using TE_{01n} ($n = 1,2$) resonators.[1]: $\varepsilon_r = 18.5$ and $\tan\delta = 1.9 \times 10^{-4}$ corresponding to $\tan\delta = 2 \times 10^{-5}$ at 1 GHz assuming that $\tan\delta \propto f$. Therefore, this material complies with all the requirements described above.

The quality of the electrode metallisation has a profound effect on the radiation efficiency. In the above calculations, for $\varepsilon_r = 20$ the efficiency η drops from 0.7 to 0.5 (corresponding to a depression by −1.8 dB) by lowering the conductivity of the metallisation by an order of magnitude (cf. Fig. 1). This demonstrates that only highly conductive metal pastes can be used for antennas with high efficiency values. We have used a metal paste made of pure silver with a dc-conductivity of 3.0×10^7 S/m.

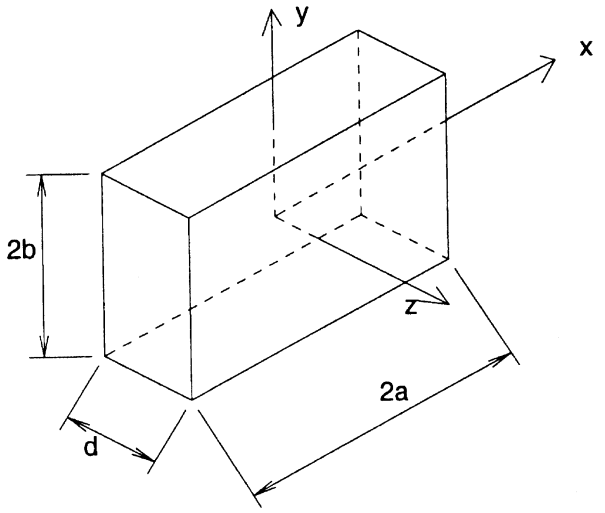

Fig. 2. Geometry of the dielectric resonator antenna (2a×2b×d).

3. Dielectric resonator antenna (DRA)

A dielectric resonator consists of a block of dielectric material. Various shapes are possible. The physical dimensions of the dielectric block determine its resonance frequencies. Due to the ease of manufacture we have investigated dielectric resonators of cuboidal shape (size $2a \times 2b \times d$, cf. Fig. 2). Fig. 3a shows the field pattern for the commonly used TE_{011} mode. We have concentrated on further miniaturisation of the DRA by means of metallising certain planes of the resonator which can act as mirror planes. Generally, metallising planes where the electric field is perpendicular to the plane does not alter the resonance frequency. Therefore, we can immediately take one quarter of the TE_{011} resonator and metallise two faces as displayed in Fig. 3b (2M-DRA). This implies that we have maintained the same resonance frequency of the resonator although we use only a quarter of the original dielectric volume. We have further minuaturised the DRA by examining further curved mirror planes inside the 2M-DRA. Fig. 4 shows several possibilities for given b and a. h will be the ultimate resonator height and the shaded area corresponds to the cross-section of the antenna. Obviously, a curved surface will be difficult to manufacture. It can be shown that for $b \to \infty$ the curved surface can be replaced by a flat one and the resonator becomes a dielectric cuboidal block metallised on three sides (see Fig. 5). We call this structure a 3M-DRA. The electromagnetic field shows that this resonator houses a quarter wavelength.

We have performed analytical calculations based on the cavity model[2] to calculate the resonance frequency,

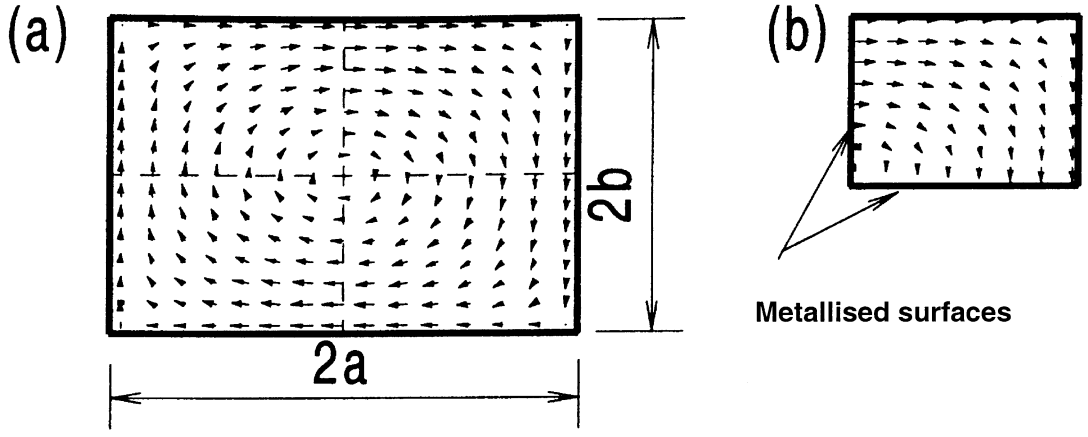

Fig. 3. (a) Field pattern of TE_{011} dielectric resonator, (b) taking one quarter and metallising two faces results in the same resonance.

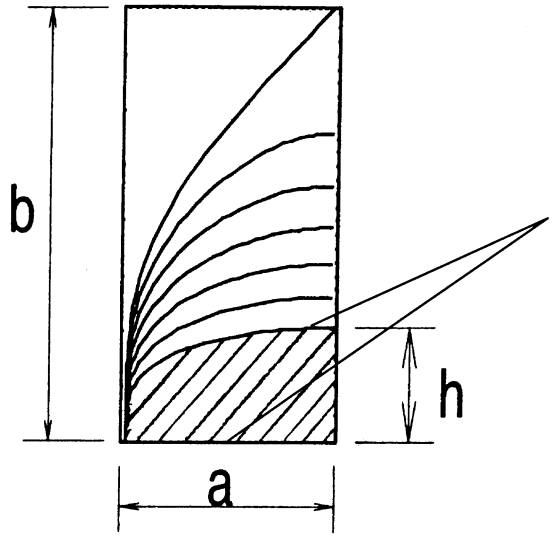

Fig. 4. Curved mirror planes for given a and b. h Corresponds to the resonator height.

bandwidth and radiation efficiency. At 1.8 GHz, we expect $\eta > 0.9$ for $\sigma > 10^7$ S/m.

We have fabricated and tested 3M-DRA's for operation at 1.8 GHz. We have realised two sizes: $10.5\times5.0\times6.0$ mm^3 (type J) and $10.5\times5.0\times4.0$ mm^3 (type K). The excitation of the resonance was achieved by a small feeding electrode on one of the faces of the resonator (cf. Fig. 5). By varying the length and width of the feed the coupling strength could be adjusted to achieve the desired coupling level.

The experimental characteristics of the antenna are summarised in Tables 1 and 2. One can see that the antenna with $h = 6$ mm has higher radiation losses resulting in a higher bandwidth and radiation gain. For type J, we have determined the radiation efficiency $\eta = 0.8$ using the Wheeler cap method.[3] The radiation pattern in the dominant plane is shown in Fig. 6. The radiation pattern is similar to that of a dipole oriented along the long side of the DRA.

Table 1
Return loss characteristics of DRA type J and K

DRA on test-PCB	Type J	Type K
Input impedance	50 Ω	50 Ω
Centre frequency	1.87 GHz	1.88 GHz
Bandwidth (RL. <-10 dB)	58 MHz = 3.1%	36 MHz = 1.9%

Table 2
radiation properties of DRA type J and K

Rotation in yz plane	Maximum gain	Average gain
DRA type J	−0.5 dBd	−2.5 dBd
DRA type K	−1.0 dBd	−3 dBd

In conclusion, the 3M-DRA is a highly efficient miniaturised antenna for narrow band applications. Possible application areas include PHS, WLAN, Bluetooth and DECT.

4. Shorting post patch antennas

Generally, patch antennas (cf. Fig. 1) serve as general purpose low-profile antennas in a variety of applications. For mobile applications in the frequency range around 1 GHz the length of a patch antenna operating in the fundamental mode is of the order of 35 mm for a dielectric constant of 20. We have concentrated our efforts on further miniaturisation of the patch antenna by the introduction of a shorting post connecting the patch with the ground metallisation.[4] The introduction of the shorting post leads to a shift of the static mode to

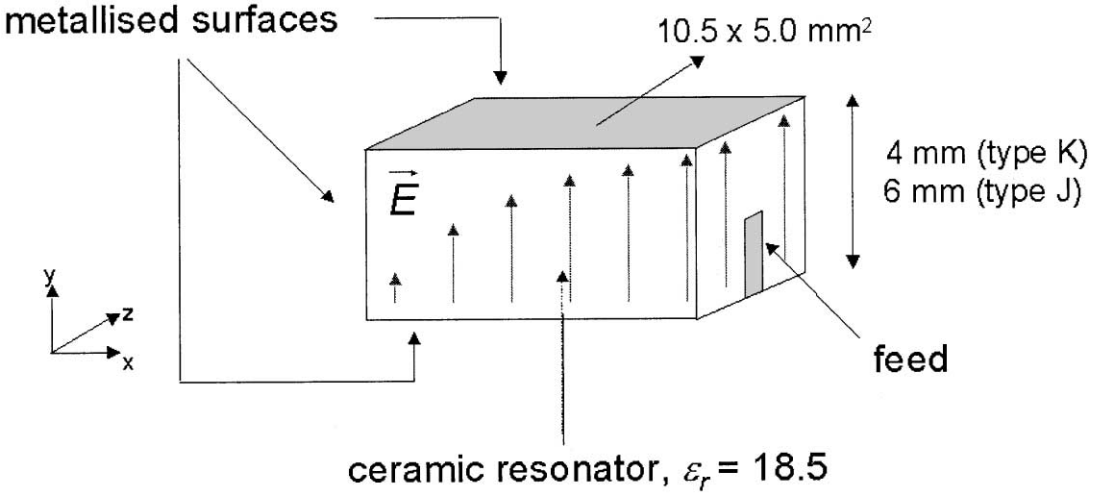

Fig. 5. 3M-DRA.

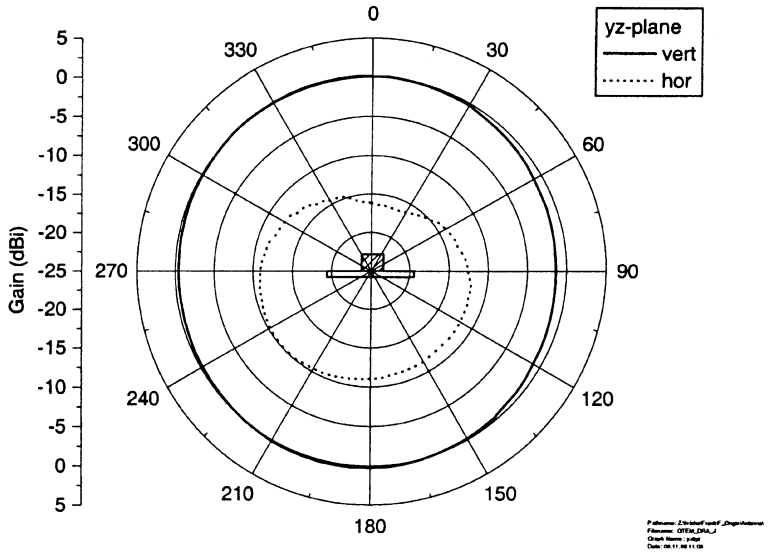

Fig. 6. Radiation of the 3M-DRA (type J) in the dominant plane.

a finite frequency below the fundamental mode of the original patch resonator. In the following, we will describe in detail our approach to calculate both the resonance frequency and the radiation properties of the antenna. For a rectangular patch the field pattern E of the shorting post antenna is constructed by a superposition of the cavity model eigenmodes e_{mn} of the same antenna without shorting post.[5] The co-ordinate origin is located at one of the corners of the resonator patch (cf. Fig. 7).

$$E(x, y) = E_z(x, y) = \sum_{m,n} A_{mn} e_{mn}(x, y)$$

with the integers $n, m \geqslant 0$ and

$$e_{mn}(x, y) = \frac{\chi_{mn}}{\sqrt{\varepsilon abh}} \cos(k_n x)\cos(k_m y),$$

$$k_n = \frac{n\pi}{a}, \quad k_m = \frac{m\pi}{b},$$

$$\varepsilon = \varepsilon_r \cdot \varepsilon_0, \quad \mu = \mu_r \cdot \mu_0$$

and

$$A_{mn} = \frac{i\sqrt{\mu\varepsilon}k}{k^2 - k_n^2 - k_m^2} \iiint_V J e_{mn} \mathrm{d}V, \; k = \omega\sqrt{\mu\varepsilon}.$$

Here, a and b denote the length and width of the resonator and h its height. ε_r and μ_r are the permittivity and the permeability of the material. χ_{mn} is a normalising factor for the eigenmodes of the unshorted patch resonator and equals 1 for $m = n = 0$, $\sqrt{2}$ for $m = 0$ or $n = 0$ and 2 for $m \neq 0$ and $n \neq 0$. J is the vertical current distribution on the shorting post. The cross-section of the shorting post is best approximated by a square (length $= \Delta$, located at (x_0, y_0) then $J = I/\Delta^2$ with I being the total current on the shorting post. Consequently,

$$A_{mn} = \frac{i\sqrt{\mu\varepsilon}k}{k^2 - k_n^2 - k_m^2} \frac{\chi_{mn}}{\sqrt{\varepsilon abh}} \frac{I}{\Delta^2} \int_{x_0-\frac{\Delta}{2}}^{x_0+\frac{\Delta}{2}} \mathrm{d}x \cos(k_n x) \times \int_{y_0-\frac{4}{2}}^{y_0+\frac{4}{2}} \mathrm{d}y \cos(k_m y),$$

which can be simplified to

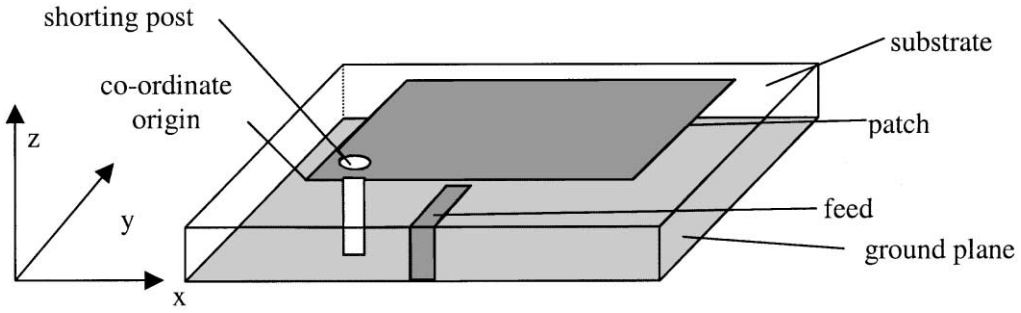

Fig. 7. Shorting post patch antenna.

$$A_{mn} = iI\sqrt{\frac{\mu h}{ab}}\frac{k\chi_{mn}}{k^2 - k_n^2 - k_m^2}\cos(k_n x_0)\cos(k_m y_0)G_{mn}$$

with

$$G_{mn} = \frac{4}{k_n k_m \Delta^2}\sin\left(k_n\frac{\Delta}{2}\right)\sin\left(k_m\frac{\Delta}{2}\right).$$

The resonance frequencies of the shorting post resonator can be found by setting E_z to zero at the position of the shorting post. This renders an implicit equation as the angular frequency ω enters the expression for E_z via k.

Once the resonance frequencies have been evaluated the electromagnetic fields inside the cavity can be calculated and the far field radiation pattern can be calculated using the cavity model. In the far field zone, the resulting vector potential due to the magnetic currents on the four non-metallised surfaces of the resonator is calculated from the general equation

$$\vec{A}_m(\vec{r}) = \frac{\varepsilon_0}{4\pi r}e^{-ik_0 r}\int_V \vec{J}_m(\vec{r})e^{ik_0 \vec{a}_r \vec{r}'}\mathrm{d}^3 r',$$
$$\vec{a}_r = \vec{r}/r.$$

Here, the magnetic current J_m is calculated from the tangential electric fields on the cavity side walls. Let $\vec{n}$ be the (outwardly directed) normal vector of these faces, then

$$\vec{J}_m = -\vec{n} \times \vec{E} = \hat{z} \times \vec{n}\cdot E_z,$$

as the electric field inside the resonator only has a z-component. The far fields are calculated from

$$E_\theta = -i\omega Z_0 A_{m\phi}$$

$$E_\phi = i\omega Z_0 A_{m\theta}$$

$$H_\theta = -E_\phi/Z_0$$

$$H_\phi = E_\theta/Z_0$$

$Z_0 = \sqrt{\mu_0/\varepsilon_0}$ is the free space wave impedance. The Poynting vector $\vec{S}$ is obtained from

$$\vec{S}(\theta,\phi) = \frac{1}{2Z_0}\left[|E_\theta|^2 + \left|E_\phi\right|^2\right]\vec{e}_r.$$

By integrating the Poynting vector over the whole sphere the radiated power can be evaluated:

$$P_{\mathrm{rad}} = \int_0^\pi\int_0^{2\pi} S(\theta,\phi)r^2\sin(\theta)0\phi\mathrm{d}\theta.$$

The antenna directivity is given by

$$D(\theta,\phi) = \frac{4\pi S(\theta,\phi)r^2}{P_{\mathrm{rad}}}.$$

In order to calculate the antenna efficiency and gain the quality factors for the individual loss mechanisms (radiation, ohmic losses and dielectric losses) have to be evaluated. Generally,

$$Q = \frac{\omega W}{P},$$

with W being the stored energy and P being the dissipated power. Generally, at resonance the electrical energy equals the magnetic energy. Thus W can be calculated from

$$W = \frac{\varepsilon}{2}\int\int\int_V \left|\vec{E}\right|^2 \mathrm{d}V,$$

with V being the resonator volume ($a \times b \times h$).

The dissipated power originating from ohmic losses P_{cond} originates from microwave currents on the electrodes (patch and ground plane) P_{cond1} and from microwave currents on the shorting post P_{cond2}. P_{cond1} can be evaluated in the following way:

$$P_{\mathrm{cond1}} = 2\cdot\frac{R_s}{2}\int_0^b \mathrm{d}y\int_0^a \mathrm{d}x\left|\vec{H}\right|^2.$$

The magnetic field $\vec{H}$ can be calculated from the electric field via Faraday's law. P_{cond2} is obtained from integrating the surface currents on the surface of the shorting post. Dielectric losses have been neglected in the calculation. Figs. 8–10 show the variation of the resonance frequency, antenna Q and gain as a function of the shorting post position for a shorting post diameter of 0.5 mm. The antenna size is $17 \times 8.5 \times 4$ mm^3. Due to the symmetry of the problem the calculations have only been carried out for a variation of the shorting post position within one quadrant of the patch. The conductivity of the metallisation was assumed to be 3.0×10^7 S/m. The calculations have been carried out with $m_{\max} = n_{\max} = 200$ in the above equations. A further increase of $n_{\max}$ did not alter the results.

One can see from Fig. 8 that positioning the shorting post at the corner of the patch minimises the resonance frequency for given patch dimensions and shorting post diameter. The antenna Q and maximum gain $G_{\max}$ also vary as a function of the shorting post position (cf. Figs. 9 and 10). Efficiency and gain minima are found

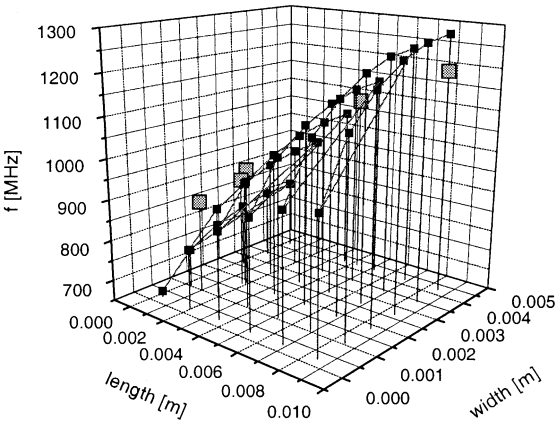

Fig. 8. Computed (black) and experimental (grey) resonance frequency as a function of the shorting post position for a shorting post diameter of 0.5 mm. The origin (0, 0) marks one corner of the patch.

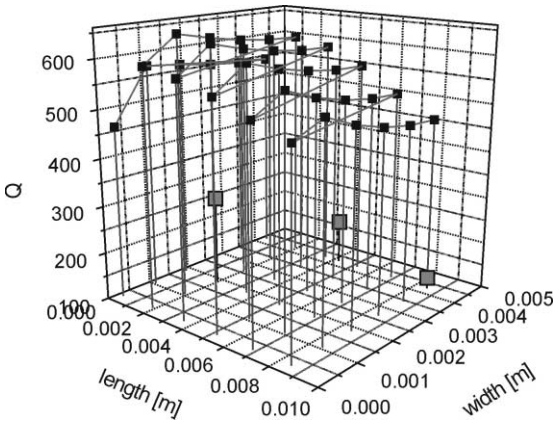

Fig. 9. Computed (black) and experimental (grey) antenna quality factor as a function of the shorting post position for a shorting post diameter of 0.5 mm. The origin (0, 0) marks one corner of the patch.

when the shorting post is inserted at the corner of the patch and at the centre of the patch. Therefore, a compromise between the degree of miniaturisation and the gain performance of the antenna has to be found. By lowering the shorting post diameter from 0.5 to 0.2 mm

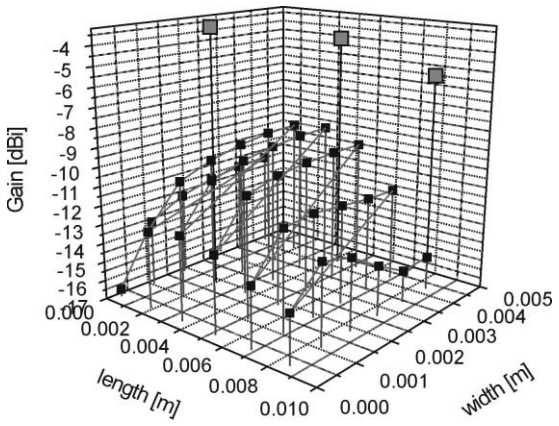

Fig. 10. Computed (black) and experimental (grey) gain as a function of the shorting post position for a shorting post diameter of 0.5 mm. The origin (0, 0) marks one corner of the patch.

the resonance frequency at fixed shorting post position is lowered by 150 MHz. Also, the gain is being lowered by approx. 4–5 dB. We have incorporated the experimental results of four shorting post antennas with varying shorting post position. The antennas were measured in an anechoic chamber. For the experiments the antenna was soldered to a coaxial stripline launcher (see Fig. 11). Its centre conductor was soldered to the antenna feed and its ground was soldered to the antenna ground.

It is apparent that the variation of the resonance frequency as a function of the shorting post position is similar to the theoretical predictions. Also, the existence of a gain minimum for a placement of the shorting post at the centre of the patch has been verified experimentally. The experimentally measured absolute gain values, however, are around 5 dB higher than the calculated ones. Also, the experimentally measured values for the antenna quality factor Q are always smaller than the theoretically predicted values (cf. Fig. 9) indicating that the total loss is higher than in the calculations. In combination with the discrepancy of the gain values this indicates that the experimental radiation losses are higher than the calculated ones. The discrepancy might

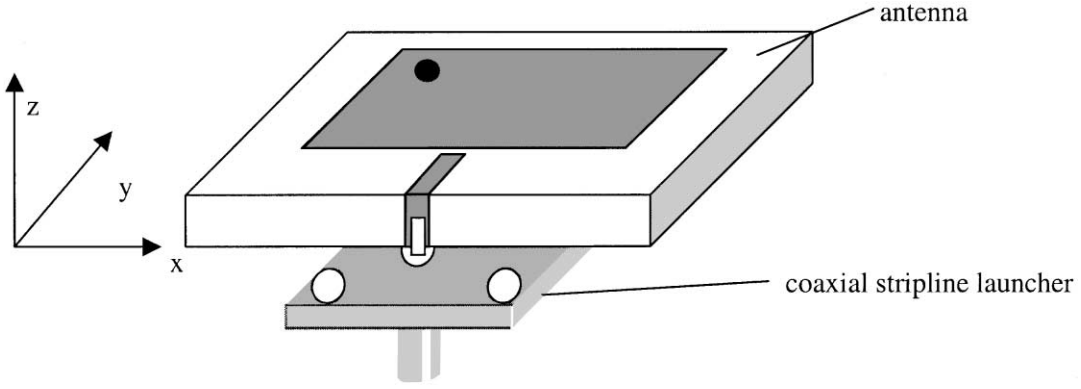

Fig. 11. Experimental setup for measurements of the isolated antenna.

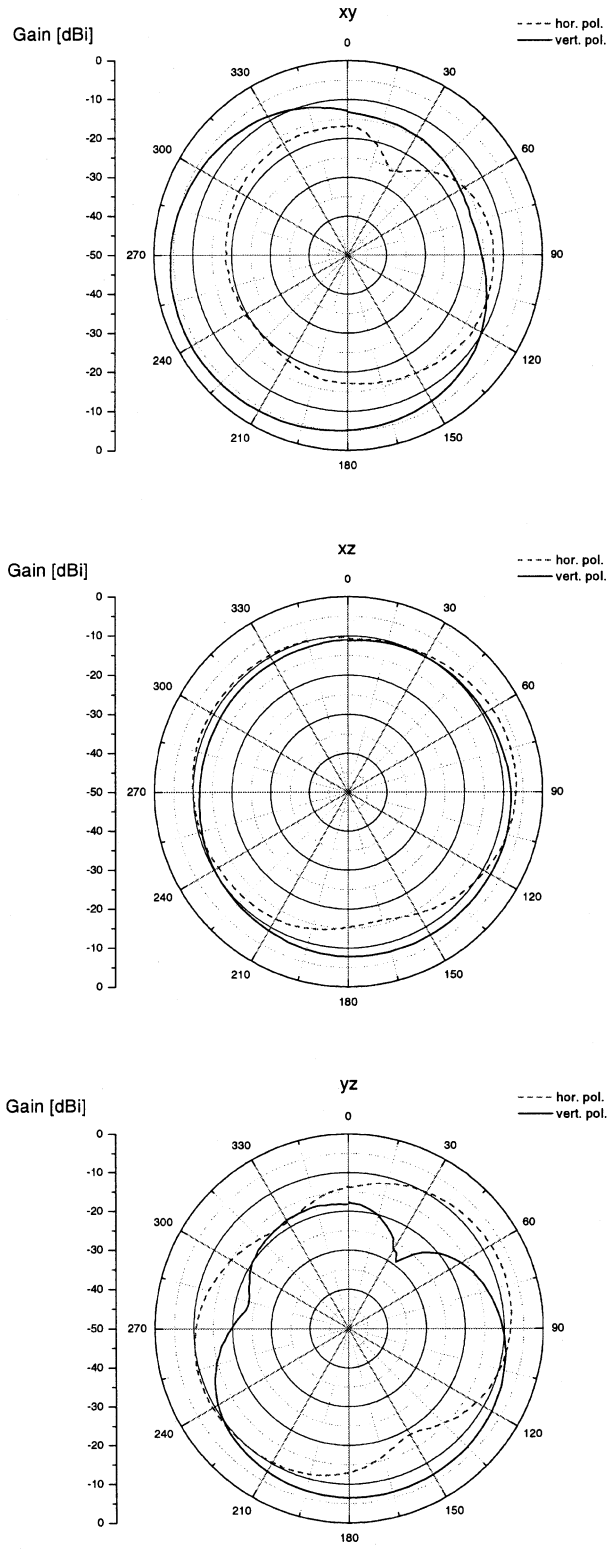

Fig. 12. Experimental radiation patterns for the isolated antenna.

originate from the crudeness of the perfect magnetic conductor boundary condition used for the dielectric—air interfaces in the framework of the cavity model.

From the above calculations we concluded that a shorting post diameter of 0.5 mm inserted at a distance of (1.9 mm, 1.9 mm) from the corner of the patch is expected to render a miniaturised shorting post antenna with a high radiation gain. We have fabricated the antenna by mechanically drilling a hole into the ceramic. A silver wire (0.5 mm dia.) was inserted into the hole and soldered to both the patch and ground metallisation. The experimental quality factor of this antenna is 240 corresponding to a 10 dB bandwidth of 3 MHz. When operating the antenna on a PCB whose size is 100×50 mm^2 the bandwidth increased to 8 MHz. This effect is generally observed for antennas placed on large PCB's and can be assigned to a larger effective volume for the electrical currents causing the antenna far field radiation.[6]

The gain measurements for the isolated antenna are displayed in Fig. 12. The maximum gain value of -3 dBi is measured in the *xy*-plane.

As demonstrated in the literature[7] multilayer of shorting post antennas can be employed to enhance the antenna bandwidth. Employing this procedure antennas for cellular applications like GSM can be approached.

5. Conclusions

We have described our approaches towards efficient miniaturised ceramic microwave antennas. Based on the key antenna parameters we have deduced the requirements for both the ceramic material used as building block of the antenna and the metallisation. Two antenna types have been introduced: the dielectric resonator antenna at 2 GHz and the shorting post antenna at 1 GHz. We have focused on maintaining a high radiation efficiency in the course of the miniaturisation process. Both antennas are suited for narrow bandwidth applications. For broadband applications (e.g. GSM) multilayer techniques can be employed to stack several antennas on top of each other.

References

1. Kobayashi, Y. and Masayuki, K., Microwave measurement of dielectric properties of low-loss materials by the dielectric rod resonator method. *IEEE-MTT,* 1985, **33**, 586–592.
2. Lee, K. F. and Dahele, J. S., Characteristics of microstrip patch antennas and some methods of improving frequency agility and bandwidth. In *Handbook of Microstrip Antennas,* Vol. 1. Peter Peregrinus, 1989, pp. 111–218.
3. Wheeler, H. A., The radiansphere around a small antenna. In *Proc. IRE*, 1959. pp. 1325–1331.
4. Waterhouse, R., Small microstrip patch antenna. *Electronics Letters,* 1995, **31**, 604–605.
5. Porath, R., Theory of miniaturized shorting-post microstrip antennas. *IEEE Tans. Ant. Prop.,* 2000, **48**, 41–47.
6. Chu, L. J., Physical limitations of omni-directional antennas. *J. Appl. Phys.,* 1948, **19**, 1163–1175.
7. Waterhouse, R. B., Broadband stacked shorted patch. *Electronics Letters,* 1999, **35**, 98–100.